Floating Floor Attenuation of Impact Structure-borne Sound in Timber Construction

A thesis submitted in partial fulfillment of the requirements for the degree of Master of Science at George Mason University

By

Nouri Hacene-Djaballah
Bachelor of Science
George Mason University, 2007

Director: Dr. Girum Urgessa
Department of Civil, Environmental, and Infrastructure Engineering

Spring Semester 2009
George Mason University
Fairfax, VA

DEDICATION

To my parents, who sacrificed everything to deliver opportunity to their children.

TABLE OF CONTENTS

LIST OF TABLES

LIST OF FIGURES

LIST OF ABBREVIATIONS/SYMBOLS

BEM	Boundary element method
FEM	Finite element method
MDOF	Multiple degree-of-freedom
SDOF	Single degree-of-freedom
SEA	Statistical energy analysis
WM2D	Working Model 2D®
c	Damping coefficient
F	Excitation (Driving) force
F_d	Damper force
F_F	Force transmitted to the foundation or load-bearing floor
F_s	Spring force
k	Spring constant
k_{eq}	Equivalent spring constant
m	mass
R_E	Impact sound reduction
V	Ratio of variables before and after adding resilient layer
$\underline{x}$	Imaginary amplitude of displacement
$x, \dot{x}, \ddot{x}$	Displacement, velocity, acceleration

ω	Excitation frequency
ω_n	Resonance frequency

ABSTRACT

FLOATING FLOOR ATTENUATION OF IMPACT STRUCTURE-BORNE SOUND IN TIMBER CONSTRUCTION

Nouri Hacene-Djaballah, MS

George Mason University, 2009

Thesis Director: Dr. Girum Urgessa

The transmission of footfall-excited impact sound is commonly reduced using floating floors. The most basic of these constructions contains three layers – a resilient material, a load-bearing floor, and a floating slab.

According to a literature review, a single degree-of-freedom (SDOF) vibration isolation model theoretically predicts impact sound reduction when assuming harmonic loading and a rigid load-bearing floor. However, for timber layers excited by transient loading (e.g. footsteps), sound reduction estimations may contain uncertainties due to inadequate modeling of footsteps and/or floor components. Therefore, this research presents a technique for modeling timber floating floors, as multiple degree-of-freedom (MDOF) systems, using the rigid body dynamics software Working Model 2D® (WM2D).

WM2D is first used to verify the SDOF case, by comparing software-generated impact sound reduction plots to graphs found in the literature. Results show agreement

between both sources, though with slight error in predicting resonance values. Next, an MDOF model is created with a transversely orthotropic and flexible timber load-bearing floor along with mechanical systems representing the footstep and resilient layer. The impact sound reduction graph for the MDOF system achieves higher values than the SDOF case, which can be attributed to additional resiliencies from flexible beams. Also, regions within the graph resemble the sound reduction plot for the SDOF case.

CHAPTER 1 Introduction

Structure-borne sound caused by footfall is one of the many potential vibration problems in buildings. This phenomenon occurs when footsteps produce mechanical floor oscillations which transmit to other structural components, causing sound radiation (Möser 2004).

The most obvious way to reduce sound radiation is to prevent its occurrence at the source (Natke and Saemann 1995). This is implausible for footfall excitation due to the variety and unpredictability of human walking characteristics (Ekimov and Sabatier 2006). Therefore, the best approach is to hinder oscillation transmission using attenuation measures, such as the commonly employed floating floor.

Basic floating floors consist of an insulating resilient layer placed between a floating slab and a rigid concrete load-bearing floor. This translates into a single degree-of-freedom [SDOF] vibrating system, with the resilient layer modeled as a spring and the slab as a mass. A damper may be included to represent any material losses, which cause the loss of sound through absorption.

When loaded harmonically at an excitation frequency near the system's natural frequency, resonance occurs and the system exhibits detrimental vibration amplitudes and amplification of the impact sound. At frequencies smaller than the natural frequency, the

SDOF floating floor provides no sound level reduction. Therefore, to achieve attenuation of impact sound, the resonance frequency must be made as low as possible. One way to decrease the resonance frequency is to increase the mass of the floating slab by using concrete. However, in residential construction, the use of lightweight timber is a more preferable option (Natke and Saemann 1995, Meirovitch 2001, Möser 2004).

When using timber for the floating slab and load-bearing floor, a SDOF assumption is no longer valid. In this case, a multiple degree-of-freedom [MDOF] system can be implemented to model timber's innate attenuation capabilities and orthotropic nature. Also, utilizing a harmonic forcing function does not accurately represent the transient nature of a footstep. Therefore, the purpose of this thesis is to develop a MDOF model for vibration isolation of floating floors under transient loading conditions. Due to its complex nature, the MDOF model will be created in Working Model 2D® (WM2D) – a rigid body dynamics software – using dimensions and material properties obtained from previous research efforts in the literature.

This thesis is split into two main sections. The first is a literature review of existing floor attenuation models for impact structure-borne sound. Topics covered include source modeling, prediction methods in impact sound insulation, standard and floating floor constructions, and vibration isolation.

The second section focuses on vibration isolation and begins with a closed-form derivation of the SDOF floating floor case. The purpose of this derivation is to show the

link between structural dynamics and acoustics, relating terms obtained by vibration isolation analysis to those which quantify impact sound reduction. Additionally, this derivation is used to calibrate WM2D by comparing software-generated plots of impact sound reduction to those found in the literature. Once the SDOF case is verified, a MDOF model is created and analyzed. The main objective of the MDOF model is to replace idealizations present in the SDOF system with more detailed sub-models. For example, the rigid concrete foundation is replaced with a compliant and transversely orthotropic timber load-bearing floor. The final step in the MDOF analysis is to compare the impact sound reduction graph to the SDOF case.

The thesis concludes with a discussion of contributions to the areas of structural dynamics and acoustics, as well as the advantages and disadvantages of using WM2D for the prediction of impact sound reduction. Potential areas for future work are also identified.

CHAPTER 2 Literature Review

This chapter begins with an overview of two major impact sound sources, human footsteps and tapping machines, followed by a discussion on impact sound prediction methods. Studies applying these methods are then introduced beginning with standard floor constructions and progressing towards floating floors. The review of floating floor configurations starts with simplified models containing rigid concrete load-bearing floors and continues to timber-only structures. The literature review ends with a more detailed look at vibration isolation as it relates to impact sound reduction. An introduction to double floating floors is also included.

2.1 Modeling the Source

The excitation source provides the load which drives a system undergoing vibration. In the case of walking impact sound, the source must accurately represent a human footstep. In theory, human footsteps cause transient forces that are non-periodic at a point, yet periodic along a given axis. According to Brunskog and Hammer (2000), footfall on floors can be described as time-periodic impacts of rigid masses. If assuming a linear floor system, the source is better described using a transfer function in the form of a Dirac pulse or time harmonic. The impact noise level can then be found by dividing the transfer function by the force spectrum of a tapping machine. This machine, shown in

Figure 2, is a standardized form of impact sound measurement which contains a horizontal row of hammers of various masses that impact floors at very low frequencies of around 5-10 Hz (Warnock and Fasold 1998, Möser 2004).

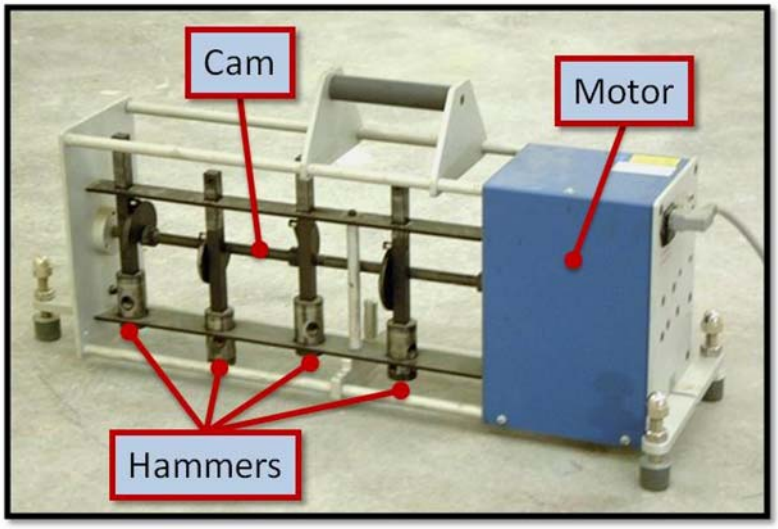

Figure 1 – Tapping Machine with Parts Labeled
Source: www.sp.se

2.1.1 The Tapping Machine

Though standardized as a form of impact sound measurement, Scholl and Maysenhölder (1999) recognized the tapping machine's shortcomings in representing human footsteps. They began by modeling interactions among the impact source, floor covering, and load-bearing floor as a mechanical system in which a free-falling mass (foot or hammer) impacts a spring (floor covering) attached to a larger mass (load-bearing structure), creating a temporary mass-spring-mass system. The authors concluded that sound radiation properties and impedance (force over velocity) of the source and

floor influence the received impact magnitude. As such, the standard tapping machine does not imitate the human source properly, and should be modified.

As a result, Scholl (2001) developed and tested a modification to the standard tapping machine, enabling it to mimic the source mechanical impedance of a human walker more accurately. This was accomplished by first measuring the impedance of walkers in both seated and standing positions. Next, the walker was replaced by a modified tapping machine composed of masses and five layers of a resilient rubber cork material. In order to assess the modified tapping machine, it was tested against the human walker and the standard tapping machine on two floors, one of timber joist construction and the other of solid concrete.

The author determined that the modified tapping machine provided greater agreement with walkers based on impact sound pressure spectra data and weighted impact sound pressure levels. Additionally, the modified machine acted similarly on both tested floor surfaces, potentially showing that the new machine may provide results independent of floor type and configuration. The study, however, did not investigate results on floating floors or floors with soft coverings. Additionally, the author acknowledges that including the entire weight of the walker in the analysis may alter the results.

2.1.2 Human Footsteps

As further proof of the intricacies of human-induced floor vibrations, Ekimov and Sabatier (2006) investigated the vibration and sound signatures of human footsteps on

concrete ground floor of a building. Measurements from both accelerometers and microphones reveal that acceleration is the best measure when determining the high frequency content of footsteps. This, in turn, showed that different floor coverings affect the friction between the foot and floor, changing the high frequency content of the step.

Perhaps the most relevant section for impact sound insulation was the analysis of walking styles. The authors expand on previous works in order to develop a mechanical model of a walker. They found that the force applied to the floor from the human mass-spring model is proportional to the leg stiffness. Changes in walking style changed low frequency (<500 Hz) content, but produced smaller changes in the high frequencies.

2.2 Prediction Methods in Impact Sound Insulation

Wachulec et al. (2000) presented a review of various methods used in the prediction of structure-borne noise radiation. The wave approach assesses wave propagation by establishing systems of equations and associated boundary conditions. If an analytical solution cannot be found, the problem is discretized using numerical methods such as the Finite Element Method [FEM] or Boundary Element Method [BEM]. These methods are accurate in the low frequencies, but they will begin to deteriorate in the high frequencies as modal parameters become less accurate. To overcome this, statistical methods including Statistical Energy Analysis [SEA] are utilized. The authors end the review by addressing methods applicable to the middle

frequencies, those frequencies at which FEM is inaccurate and SEA assumptions are not yet fulfilled. As a result, the two methods may be combined for improved accuracy.

The wave approach, focused on wave propagation theory, was used by Tadeu et al. (2007) to predict impact sound levels for infinite homogeneous multilayer plates under point loads. The layers of the analytical formulation could be changed to have fluid or elastic properties based on the configuration under investigation. Material properties required for fluid layers were density, Lamé constants, and dilatational wave velocity. Elastic layers were characterized by density, Young's Modulus, Poisson's ratio, compressional wave velocity, and shear wave velocity.

For each layer, series of equations were obtained by deriving potentials, stresses, and displacements at interfacing surfaces. These equations were then combined with boundary conditions to complete the analytical model. A BEM model was used to verify the model, but had limitations in its discretization due to the introduction of large amounts of damping. Internal material losses were considered using complex Young's modulus and complex Lamé constants.

A single concrete layer and a suspended ceiling construction composed of concrete, air, mineral wool, and plaster were tested to validate the analytical model. For the suspended ceiling example, resonances excited in the air gap create multiple sharp increases in impact sound pressure levels above 1000 Hz. The ceiling was tested in three configurations: empty air gap, filled air gap, and partially filled air gap. The authors did not analyze timber floor configurations, as the model dealt only with homogenous plates. Timber may be incorporated by altering material property and wave velocity values.

2.3 Floor Constructions

2.3.1 Standard

Standard constructions, an example of which is shown in Figure 2, consist of slabs placed directly on load-bearing floors or supports. Brunskog and Hammer (2000) conducted a review of deterministic prediction models for impact sound insulation in timber standard floors composed of infinite and finite plates and beams. A focus was placed on periodic structures, in which periodicity existed in both geometry and exciting force. Nearly periodic structures, those which contain small irregularities, were also investigated. The authors found that the Fourier transform holds the largest applicability across the various models studied, useful for both point forces and sound radiation.

Figure 2 – Standard Timber Floor (Slab on Load-Bearing Joists)
Source: www.albengroup.com

Discrete methods have also been used in standard floor prediction models. Bard et al. (2008) sought to improve the accuracy of FEM models to predict the impact sound transmission and attenuation in standard floor constructions. Two models were investigated, one with a single chipboard plate attached to a timber joist and the other with two boards attached to the joist. The frequency range of the study was from 25 Hz to 500 Hz.

To account for the transverse orthotropic nature of timber, the chipboard plates were analytically composed of five layers, the outer two using one elastic modulus and the inner three using a separate one. The timber joists also had different elastic moduli both transversally and longitudinally. The metal screw fasteners, which connect the chipboard plates to the spruce beams, were modeled as a column of discrete elements assigned to steel properties. The chipboard-beam interface was modeled using springs with differing damping coefficients based on the proximity to the metal screws. In this model, a complex elastic modulus was used in which the loss factor was frequency dependant. Additionally, impact locations were assumed to be either in the bay or directly on the joist.

The FEM model was verified experimentally by measuring the transmission loss as a function of velocity changes and vibration reduction levels. The authors concluded that attenuation of wave propagation is frequency-dependant, with discontinuities causing more pronounced wave velocity reduction. A good agreement was present between the experimental and FEM model results.

The addition of soft floor coverings on standard floors was investigated by Scholl and Maysenhölder (1999). The authors used a mass-spring-mass model to calculate the impact force reduction after installing carpet on floors of infinite and definite mass, impacted by various hammer sizes. Results demonstrated that the impact source, floor covering, and base floor have strong influence on achieved force reduction. They also noted that non-linear effects from carpets under large loads or from round impact hammers should be taken into account, as such effects may influence insulation in practical applications.

2.3.2 Floating Floors

A basic floating floor consists of three parts: a "floating" slab, a resilient layer, and a rigid load-bearing floor. Figure 3 shows a floating floor with both a concrete floating slab and a concrete load-bearing floor. According to a survey conducted by Wuyts et al. (2006), using timber instead of concrete for floating slabs is more practical because timber is able to achieve the same or better insulation with much less weight. Therefore, floating floors made with concrete floating slabs are not covered in this thesis.

Figure 3 – Floating Floor with Concrete Slab and Concrete Load-Bearing Floor
Source: www.soundservice.co.uk

The most common floating floor type investigated was timber floating slabs on concrete load-bearing floors. Based on this floor type, Stewart and Craik (2000) developed a wave model for the prediction of bending wave transmission between parallel plates connected by resiliency. Their results showed that the wave model using SEA is not applicable at high frequencies or with very soft resilient layers, as coupling effects between plates become underestimated. Further, coupling effects are stronger when closed-cell foams or semi-rigid fiberglass resilient layers are used. The authors

assumed that the parallel plates are continuously connected, but this may not be the case in practice if screws are to be used.

Hopkins and Hall (2006) also focused their study on timber floating floors with rigid concrete bases. Their experiment included measuring the transmission loss of a commonly employed floating floor system in the UK. This system employs one layer of high density mineral wool with two layers of timber to provide enough structural stability. This configuration has a single-number loss of 25 dB and a resonance frequency of 119 Hz. The main purpose of their study was to find ways to increase the single-number loss to at least 29 dB.

For the resilient layer, Hopkins and Hall (2006) looked into various open cell foams as alternatives to mineral wool. According to stress-strain curve comparisons, reconstituted open cell foam (created from recycled foam) performs better than newly created foam because the former have shallower curves up to approximately 5% strain. These shallow slopes correspond to smaller Young's Modulus values and smaller stiffness values, resulting in improved sound reduction. Another benefit of reconstituted foam relating to the stress-stain curve is its much less defined yield point and yielding region in comparison to some new foams. For example, a 28 kg/m^3 new foam stressed beyond 5 kPa has a yielding region from approximately 5% to 40%. For this reason, many commercially available floating floors use open cell reconstituted foams.

The authors first measured impact sound insulation by partially covering the concrete base floor with foam and a floating floor. As a result, frequencies above 400 Hz were excited by both impact and airborne-sound. This initial testing allowed the testers to

choose one type of floating floor to fully create, using two different types of timber floating slabs. Tests show that these full-scale models achieved the desired aim of 29 dB reduction.

The final level of complexity studied for floating floors involves timber in both slabs and load-bearing floors, as shown in Figure 4. A variety of these configurations were measured by Wuyts et al. (2006) for airborne and impact sound insulation performance. The main motivation behind their study was to assess the floors' ability to meet limits imposed by future Belgian sound insulation requirements. The two values measured from the configurations were the single-number weighted sound reduction index (R_w) and impact sound insulation ($L_{n,w}$).

The authors' parametric survey revealed that floating floors without suspended ceilings do not provide enough insulation to meet the proposed new Belgian requirements. The largest insulation is realized if a ceiling is not rigidly connected to the timber joist base floor. Therefore, the best solutions have attenuation measures placed on the top and bottom of load-bearing floors.

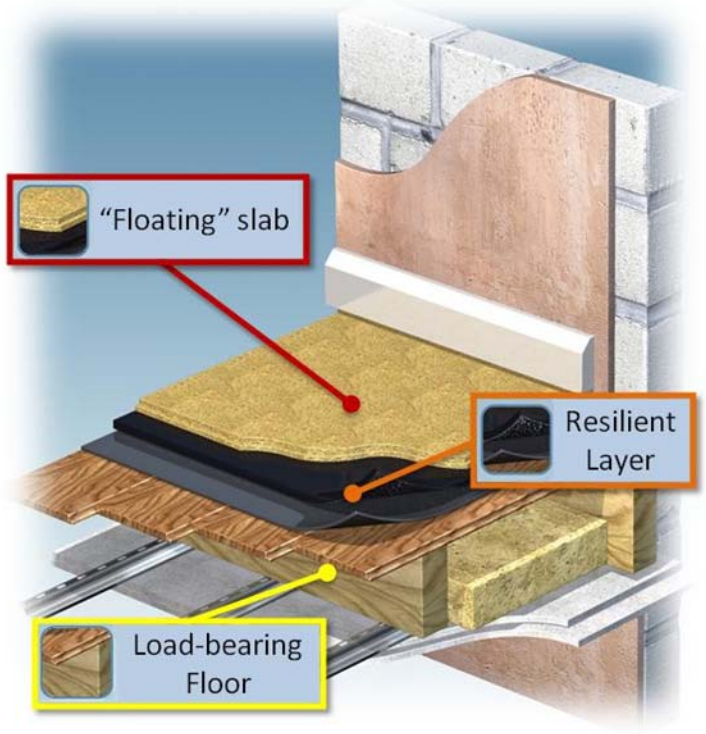

Figure 4 – Floating Floor with Timber Slab and Timber Load-Bearing Floor
Source: www.soundservice.co.uk

2.4 Vibration Isolation

The case of a rigid concrete load-bearing floor represents a mass-spring system exhibiting a single degree-of-freedom [SDOF] with the floating slab and resilient layer idealized by a lumped mass and spring respectively. The spring's stiffness, k, is proportional to the elastic modulus of the resilient layer. Many analyses assume a harmonic driving force when determining the transmission loss of floating floors. Detailed derivations of this process can be found in Möser (2004) and Blauert and Xiang (2008). Figure 5 summarizes the equivalent SDOF system.

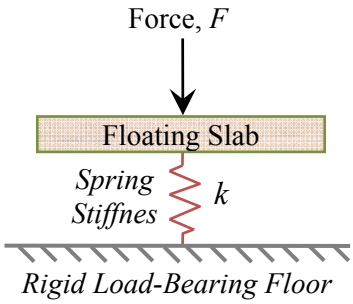

Figure 5 – Idealized SDOF Floating Floor

Hopkins and Hall (2006) discussed the trade-off between stability and insulation for SDOF floating floors. Structural stability refers to the resilient material's stiffness, whereas the insulation relates to the resonance frequency of the system. According to the analysis of a SDOF mass-spring system under harmonic excitation, the increase in stability achieved by using stiff mineral fiber requires an increase in timber mass to keep the resonance low.

The authors also investigated double floating floors, in which two floating floors are vertically layered**.** Four configurations of double floating floors were tested similarly to single floating floors without creating full-sized models. Sound insulation results were plotted along with the results of the SDOF floors. According to all measurements, using double floors decreased the adverse effects of insulation at and around the resonance frequency of the SDOF floor models. Additionally, a small slope of about 3 dB per octave existed between the two resonances, with a steep increase to about 15 dB per octave above the second resonance. This second slope is a large improvement over the 9 or 12 dB per octave usually associated with SDOF floating floors. Therefore, the major

benefit of double floating floors is that stiffer resilient materials can be used to increase structural stability, while still maintaining the improvements of a single floating floor.

Hammer and Brunskog (2002) also investigated the effectiveness of SDOF and two degree-of-freedom isolation measures for lightweight timber joist floors, but using point mobility and power approaches. They note that the receiving structure, or the load-bearing floor, should be included in the analysis for lightweight constructions.

After deriving the mobility of a periodically stiffened plate, the authors presented results for over 15 excitation positions with respect to frequency. Asymptotes representing the mobility of an infinite plate and infinite beam were then superimposed on the graph, along with vertical line asymptotes representing the frequencies at which the inverse of the peak wavelength, $1/\lambda_P$, equaled 1/4 and 1/2. The authors used these asymptotes to create two simplified graphs of mobility vs. frequency, one for excitation locations between frames and the other at/near frames. Sound pressure level measurements showed that the two-stage isolation is much more efficient in limiting sound pressures.

CHAPTER 3 – Floating Floor Analysis and Results

This chapter begins with a closed-form derivation of the basic SDOF model with rigid concrete load-bearing floor. To ensure WM2D is able to handle vibration isolation models, the software is used to obtain graphical sound reduction results for the SDOF case which are then compared to similar graphs from the literature. Next, a MDOF vibrating system composed of four sub-models – the source, the floating slab, the resilient layer, and the compliant timber load-bearing floor – is analyzed in WM2D using geometry and material properties obtained from literature.

3.1 Single Degree-of-Freedom Model

3.1.1 Closed-form derivation

The simplest vibration isolation case of floating floors is a floating slab placed on a rigid concrete load-bearing floor, as shown in Figure 6. The floating floor is modeled as a spring-mass-damper system with an applied force, *F,* and is derived as follows.

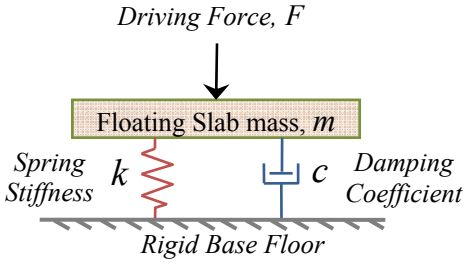

Figure 6 – Basic SDOF Floating Floor Model

The displacement of the mass is assumed harmonic (Eq. 3.1), where $\underline{x}$ represents the displacement's imaginary amplitude. The resulting velocity and acceleration are obtained through differentiation as shown in Eqs. (3.2) and (3.3) respectively.

$$x(t) = \underline{x}e^{-i\omega t} \tag{3.1}$$

$$\dot{x}(t) = v(t) = i\omega\underline{x}e^{-i\omega t} \tag{3.2}$$

$$\ddot{x}(t) = a(t) = -\omega^2\underline{x}e^{-i\omega t} \tag{3.3}$$

Summing the vertical forces on the floating slab using Newton's second law of motion gives

$$+\downarrow \Sigma F = m\ddot{x} = F - F_s - F_d \tag{3.4}$$

where the spring force, F_S, and damping force, F_d, can be expressed as

$$F_s = kx \tag{3.5}$$

$$F_d = c\dot{x} \tag{3.6}$$

Placing Eqs (3.5) and (3.6) back into Eq. (3.4) and rearranging into a SDOF motion equation gives

$$m\ddot{x} + c\dot{x} + kx = F \tag{3.7}$$

The expressions for acceleration, velocity, and displacement in Eqs. (3.1)-(3.3) can now be inserted into Eq. (3.7). If the driving force is also assumed harmonic, then the exponential terms will cancel, leaving only the complex amplitudes:

$$-m\omega^2\underline{x} + i\omega c\underline{x} + k\underline{x} = F \tag{3.8}$$

Solving for the complex amplitude of the displacement gives

$$\underline{x} = \frac{F}{-m\omega^2 + i\omega c + k} \tag{3.9}$$

The force at the foundation, F_F, is proportional to the impact sound reduction of the floating floor, and is therefore obtained next. Both the spring and damper are attached to the foundation and thus transmit a foundation force composed of both the spring and damping force

$$F_F = F_s + F_d = i\omega c\underline{x} + k\underline{x} = (i\omega c + k)\underline{x} \tag{3.10}$$

Placing Eq. (3.10) into Eq. (3.9), the foundation force becomes

$$F_F = \frac{i\omega c + k}{-m\omega^2 + i\omega c + k} F \tag{3.11}$$

Eqs. (3.1) to (3.11) represent the structural dynamics side of the impact sound problem. In order to utilize this information in an acoustics context for assessing the impact sound loss of a resilient layer, a ratio of foundation forces, *V*, is calculated. The denominator of *V* is Eq. (3.11). The numerator of *V* contains the limit of Eq. (3.11) as the spring constant approaches infinity, representing a completely rigid layer. The limit is evaluated using l'Hôpital's rule and yields

$$\lim_{k\to\infty} \frac{i\omega c + k}{-m\omega^2 + i\omega c + k} F = F \tag{3.12}$$

As a result, *V* is merely the inverse of Eq. (3.11) with the driving force, *F*, cancelled out

$$V = \frac{F}{\frac{i\omega c + k}{-m\omega^2 + i\omega c + k} F} = \frac{-m\omega^2 + i\omega c + k}{i\omega c + k} \tag{3.13}$$

The final step in obtaining the impact sound loss, R_E, in decibels is to place the ratio, V, in a logarithmic equation

$$R_E = 10\log|V|^2 \tag{3.14}$$

3.1.2 Working Model 2D® Verification

To verify the SDOF closed-form solution, the case was analyzed using the WM2D software. This tool calculates and displays the motions on rigid bodies using Newton's second law of motion. Connections between rigid bodies can be defined using springs and dampers, as well as pinned, fixed, or slotted joints. The program is also able to detect collisions and measure contact forces between bodies. Perhaps WM2D's most powerful feature is its highly customizable proprietary formula language, which allows output graphs to show virtually any user-defined function (Wang n.d.). Since the vibration isolation case of Figure 6 uses Newton's second law to derive the equation of motion, the software was deemed an appropriate tool for verifying Eq. (3.14).

The WM2D model contains two sub-models: the first connects the load-bearing floor to the floating slab with a rigid rod in order to directly transfer the applied force to the foundation (Figure 7). The second connects the floor and slab with a vertical spring-damper system (Figure 8). Both sub-models attach the load-bearing floor to the background with a rigid joint. This point serves as the measuring location for the foundation force shown in Eq. (3.11).

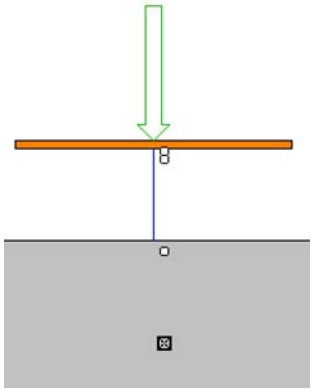

Figure 7 – Rigid sub-model

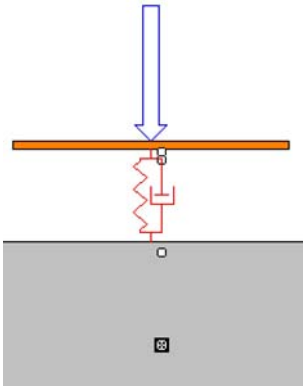

Figure 8 – Elastic sub-model

Graphs in WM2D default to the time domain, which is useful for verifying the harmonic nature of vertical displacements. However, to properly asses the sound reduction characteristics of a vibrating system, a graph of the frequency response is necessary. Therefore, the x-axis is modified with the custom formula

$$-1/time \tag{3.15}$$

signifying the excitation frequency, ω. The negative sign is required because WM2D runs models with increasing time and decreasing frequency as a default. Therefore, in order to obtain increasing frequency on the horizontal axis, negative frequency values were used. The time step in the software was set to 0.0002 seconds and progresses through frequency using Eq. (3.15) as shown in Table 1.

Time (s)	0.0002	0.0004	0.0006	0.0008	0.0010	0.0012	
1/time (Hz)	5000	2500	1666.67	1250	1000	833.33	**DECREASING**
-1/time (Hz)	-5000	-2500	-1666.67	-1250	-1000	-833.33	**INCREASING**

Table 1 – Time vs. Frequency Comparisons

After defining the horizontal axis, the foundation forces for both the rigid and elastic sub-models were formulated. Constraints in WM2D are objects which connect rigid bodies. Therefore, to refer to the force at a particular point, for instance the rigid joint which holds the load-bearing floor to the background, the syntax required is

$$|constraint[\#\#].force| \tag{3.16}$$

where the vertical bars represent magnitude and ## represents the number WM2D assigns to the constraint. The elastic foundation force is similarly defined as the absolute value difference between the applied force and the force seen as the load-bearing floor. This is to insure that both the rigid and elastic forces start at the same initial value.

According to Figure 9, the foundation force for the rigid sub-model remains constant because the connecting rod will never "absorb" the applied force. In contrast, the elastic foundation force decreases in magnitude and obtains an increasingly negative slope as the distance between the load-bearing floor and slab decreases. Resonance occurs when the applied force equals the foundation force because then the slab is forced down at the same rate as the spring pulls down, causing the detrimental displacements indicative of the resonance frequency.

The elastic foundation force in Figure 9 does not go to infinity. The actual behavior, shown in Figure 10, is shown by zooming on the upper right section of the graph, where the rigid foundation force is no longer visible. The elastic foundation force becomes constant around 245 lb, obtained from subtracting the applied force from the

force in the spring. The three spikes in the graph occur when the floating slab impacts with the load-bearing floor.

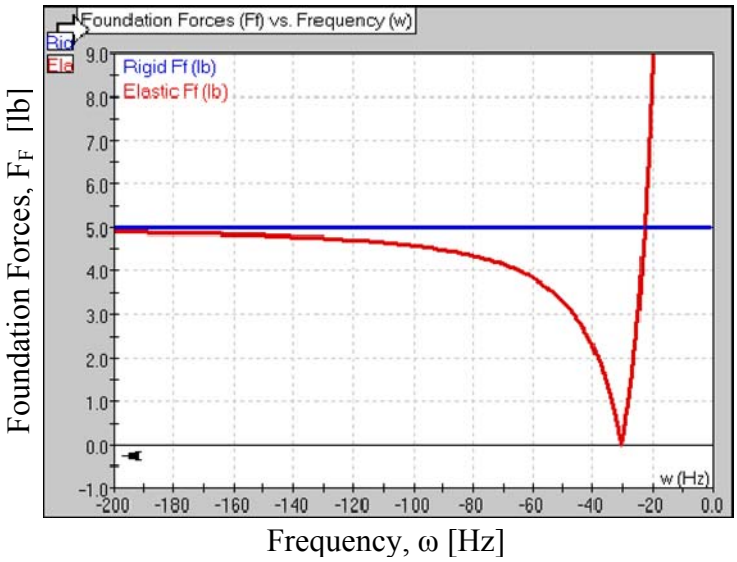

Figure 9 – Foundation Forces vs. Frequency [SDOF]

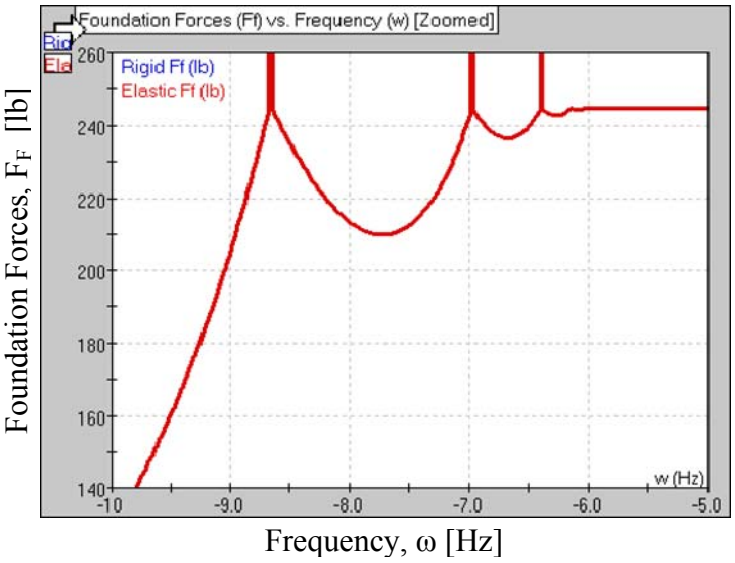

Figure 10 – Foundation Forces vs. Frequency (Zoomed) [SDOF]

The ratio V shown in Eq. (3.13) was defined in WM2D as the ratio between the elastic and rigid foundation forces. Since both forces were already inputted using Eq. (3.16), the V equation merely references values from an existing output graph using the syntax

$$output[\#\#].y! \tag{3.17}$$

where ## is the existing graph's number and ! is the cell number with the required value. For example, if the rigid and elastic forces where in cell *y1* and *y2* of output *20* respectively, the ratio V becomes

$$V = output[20].y2/output[20].y1 \tag{3.18}$$

Figure 11 shows the output graph from WM2D for the ratio V. It has a similar shape to the elastic foundation force, but instead begins at one when the forces before and after the resiliency are equal.

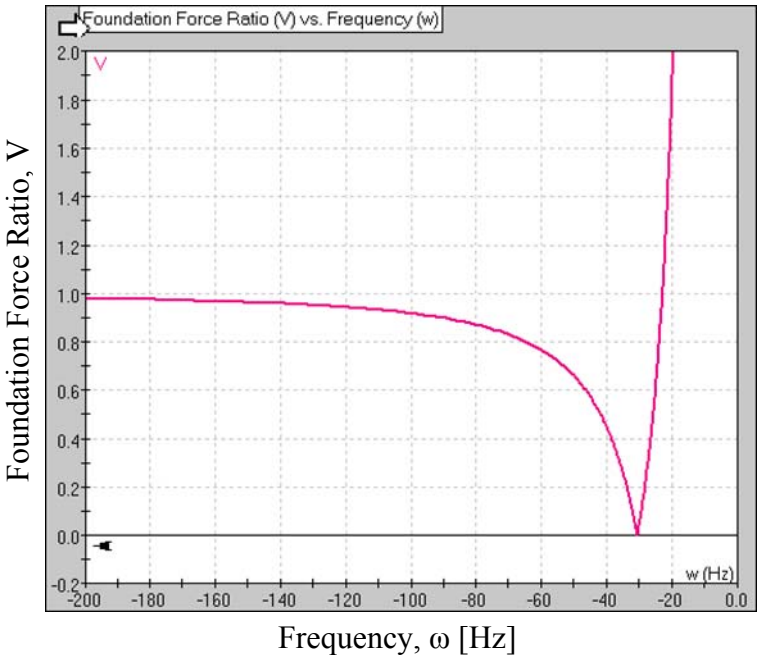

Figure 11 – Foundation Force Ratio vs. Frequency [SDOF]

The final calculated value was the impact sound reduction shown in Eq. (3.14). Following the naming conventions for graphs in WM2D, if the ratio *V* was placed in cell *y3* of output *20*, the formula to obtain the impact sound reduction becomes

$$R_E = 10 * \log(output[20].y3\text{^}2) \tag{3.19}$$

The graph of Eq. (3.19), shown in Figure 12, conforms to plots found in the literature for SDOF floating floor vibrating systems. It begins at zero when the resilient layer modeled by the spring-damper system does not provide any sound reduction benefits. At the resonance frequency, negative benefits are seen. Finally, above the resonance, the graph shows positive values signifying impact reduction (Natke and Saemann 1995, Möser 2004, Blauert and Xiang 2008).

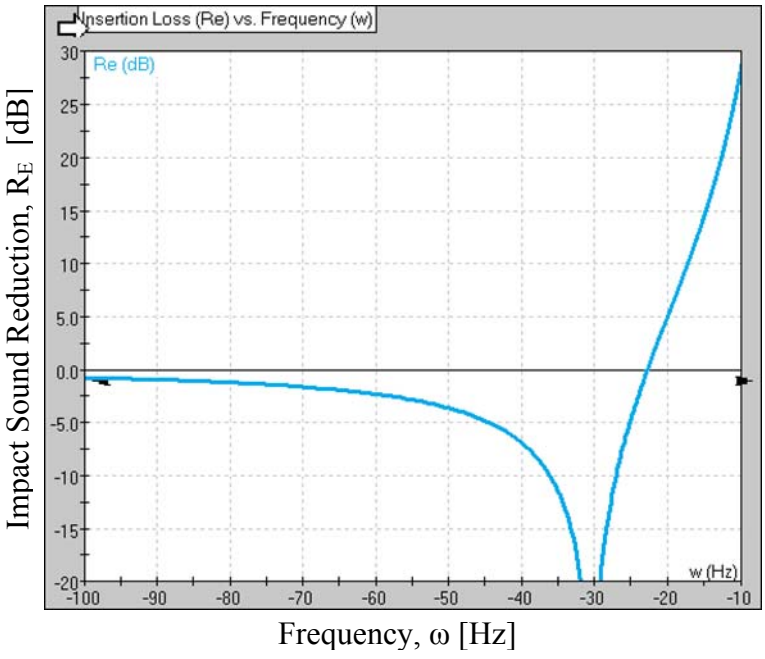

Figure 12 – Impact Sound Reduction vs. Frequency [SDOF]

While the shape of Figure 12 agrees with literature, the numerical resonance value does not. For a SDOF system, the resonance is

$$\omega_n = \sqrt{k/m} \tag{3.20}$$

where k is the spring stiffness and m is the mass of the floating slab. For the WM2D SDOF model, the spring stiffness is 50 lb/ft and the slab's mass is 0.031 slugs, corresponding to a resonance of

$$\omega_n = \sqrt{50/0.031} \approx 40\ Hz \tag{3.21}$$

However, the horizontal axis in Figure 12 shows a resonance of approximately 30 Hz. This discrepancy may be attributed to three main reasons. First, WM2D calculates model values at the discrete time step defined by the user. As a result, errors introduced early in the model can carry over to adjacent time steps and affect future graph values. Second, the impact sound reduction graph may be plotting the frequency of damped vibrations, which is a smaller value than resonance. Third, plotting the frequency domain using WM2D may be an incorrect approach. By linking to MathWorks Matlab® using WM2D's external object capabilities, a more accurate impact sound insulate graph could be produced.

Though the resonance values do not agree, the impact sound reduction graph is similar to those found in the literature for SDOF floating floors. Therefore, analysis will continue for the MDOF case.

3.2 Multiple Degree-of-Freedom Model

3.2.1 Compliant Load-Bearing Floor

In the SDOF model, the load-bearing floor was created using a single rigid rectangular body attached to the background. Rigid load-bearing floors are employed by Hopkins and Hall (2006) and Scholl and Maysenhölder (1999) to represent concrete foundations. However, for a compliant timber floor, a flexible beam approach is used instead. This is created in WM2D using the Flexbeam script, which simulates flexible beams by splitting rigid beams into a user-defined amount of elements, each of which is connected with rotational springs and dampers. When running the Flexbeam script for the first time, WM2D displays the dialog box shown in Figure 13.

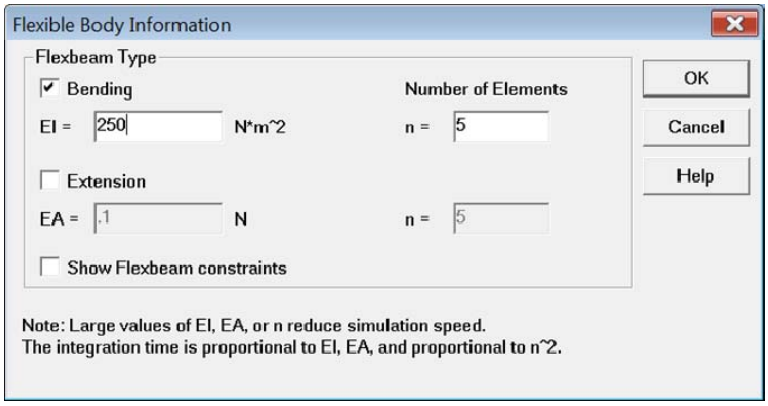

Figure 13 – Flexbeam Script Dialog Box in WM2D

This window allows both the bending stiffness, *EI*, and element number, *n*, to be inputted. Enabling the "Show Flexbeam constraints" checkbox displays the rotational springs on the model in between each element. After accepting these values, the beam's

bending stiffness and bending damping can be changed in real-time using control sliders (Wang n.d.).

The geometry and material properties of the timber load-bearing floor, shown in Table 2 and Table 3 respectively, are obtained from Bard et. al (2008). In order to model timber as a transversely orthotropic material, the floor is composed of five layers which differ in bending stiffness. The thickness of all layers is uniform at 0.005 meters, with the total thickness of the load-bearing floor becoming 0.025 meters.

Layer	**Quantity**	**Thickness** *(m)*	**Length** *(m)*	**Width** *(m)*	**Moment of Inertia, *I*** *(m^4)*
Outer	2	0.005	1.2	1.2	1.25E-08
Inner	3	0.005	1.2	1.2	1.25E-08
TOTAL	***5***	***0.025***			

Table 2 – Geometry of Timber Load-Bearing Floor

Layer	**Density, *ρ*** *(kg/m^3)*	**Young's Modulus, *E*** (k*Pa)*	**Bending Stiffness, *EI*** *($N{\cdot}m^2$)*
Outer	920	20,000,000	*250*
Inner	920	5,600,000	*70*

Table 3 – Material Properties of Timber Load-Bearing Floor

Each of these layers was created in WM2D using the Flexbeam script with ten elements each. The major challenge was to connect the individual layers and elements into one beam in order to prevent vertical separations between elements. This was

accomplished using slot joint constraints in which a point on the top of each element is attached to the slot on the bottom of the element above.

The support condition of the model is a single simply-supported span, with a pin joint on the bottom left element and a slot joint representative of a roller on the bottom right element. The complete load-bearing floor is shown in Figure 14, accompanied by a detailed view in Figure 15 with layer outlines of Flexbeam elements visible.

Figure 14 – Load-bearing Floor in WM2D

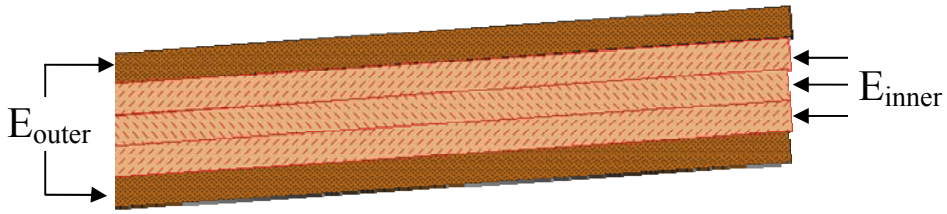

Figure 15 – Load-bearing Floor in WM2D (Detailed View)

3.2.2 Resilient Layer

Hopkins and Hall (2006) determined that sound insulation of lightweight floating floors is maximized when using a reconstituted open cell foam resilient layer with minimized dynamic stiffness. The authors obtain a minimum dynamic stiffness of 4 MN/m^3 by stacking two recycled foam layers, with the top layer 25 mm thick (7 MN/m^3) and the bottom layer 20 mm thick (9 MN/m^3).

In WM2D, these layers are treated as a single spring with an initial height of 45 mm. The equivalent spring constant, k_{eq}, was obtained by taking into account both bending stiffness, *EI*, and axial stiffness, *EA*. Young's Modulus is estimated by multiplying the dynamic stiffness in MN/m^3 by the layer thickness in meters, yielding

$$E = (4{,}000{,}000\ N/m^3) * (0.045\ m) = 180{,}000\ Pa \tag{3.22}$$

A summary of the resilient layer's geometry and material properties is shown in Table 4 and Table 5 respectively.

Layer	**Thickness** *(m)*	**Length** *(m)*	**Width** *(m)*	**Area** *(m^2)*	**Moment of Inertia, *I*** *(m^4)*
Resilient	0.045	1.2	1.2	1.44	9.1125E-06

Table 4 – Geometry of Resilient Layer

Layer	**Density, *ρ*** *(kg/m^3)*	**Young's Modulus, *E*** *(Pa)*	**Bending Stiffness, *EI*** *($N{\cdot}m^2$)*	**Axial Stiffness, *EA*** *(N)*
Resilient	80	180,000	*1.64*	*259,200*

Table 5 – Material Properties of Resilient Layer

The equivalent spring constants for various support and loading conditions in beams. For a simply supported beam loaded at midspan,

$$k_{eq} = \frac{48EI}{L^3} \tag{3.23}$$

For axial deformation of a layer,

$$k_{eq} = \frac{EA}{L} \tag{3.24}$$

The deformations due to both bending and compression act vertically, therefore Eq. (3.23) and (3.24) act in series. The equation for combining springs in series is

$$k_{eq} = \left(\sum_{i=1}^{n} \frac{1}{k_i} \right)^{-1} \tag{3.25}$$

Using information from Table 4 and Table 5, the final equivalent spring constant is calculated as follows:

$$k_{eq} = \left(\frac{L^3}{48EI} + \frac{L}{EA} \right)^{-1} = \left(\frac{(1.2)^3}{48 * 1.64} + \frac{0.045}{259{,}200} \right)^{-1} \approx 45.52 \, \frac{N}{m} \tag{3.26}$$

3.2.3 Floating Slab and Source

For simplicity, the floating slab is modeled as a rigid body similar to the SDOF case, though it too can be designed as a Flexbeam. The WM2D model of the floating slab does not include soft coverings such as carpet due to their non-linear nature (Scholl 1999). The geometry and material properties of the floating slab are taken from Hopkins and Hall (2006) and are summarized in Table 6.

Layer	Thickness *(m)*	Length *(m)*	Width *(m)*	Density, ρ *(kg/m^3)*
Floating Slab	0.022	1.2	1.2	668

Table 6 – Geometry and Material Properties of Floating Slab

The footfall source has been adapted from Scholl (2001). It consists of the modified form of the standard tapping machine, idealized into a mass-spring-mass system representative of a human walker's impedance. This mechanical system, shown in Figure 16, was placed in WM2D and populated with the constants obtained from Scholl (2001). In order to ensure that the source remained vertical during analysis, it was attached to vertical slot joints.

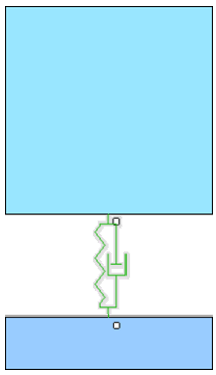

Figure 16 – The Source in WM2D

3.2.4 Impact Sound Reduction

The complete MDOF floating floor system is shown in Figure 17. Before the sound reduction can be calculated, an identical model with a rigid connection must be created. The rigid connection is simulated by assigning an arbitrary k value of 80,000 N/m, which represents a spring constant approaching infinity when compared to k_{eq} in Eq. (3.26).

Since bending (flexural) waves contribute the most to impact sound radiation (Cremer et al. 2005), the force transmitted to the load-bearing floor is measured at the

center of the bottom layer, where the flexural displacement is highest and where all layers have contributed to force reduction.

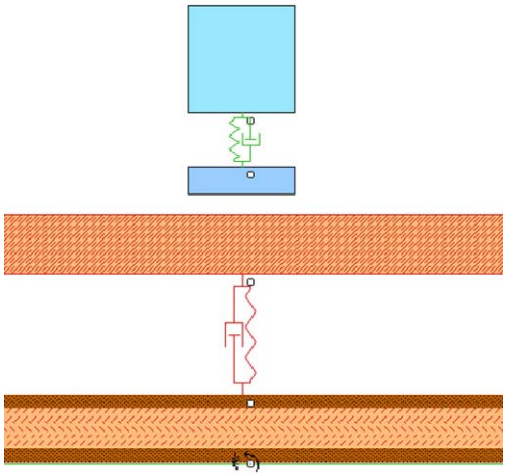

Figure 17 – Complete MDOF model in WM2D

The impact sound reduction for the MDOF system is shown in Figure 18. Upon closer inspection, various sections of this graph resemble the impact sound reduction for the SDOF case shown in Figure 12. Therefore, sharp discontinuities in Figure 18 may be indicative of resonance frequencies. Since the WM2D model contains MDOF, the negative effects at resonance frequencies should be lower than those obtained for the SDOF case. The is true for almost all locations in the graph. Additionally, the graph reaches much larger sound reductions as compared to the SDOF floating floor due to the inclusion of timber compliance in the load-bearing floor sub-model.

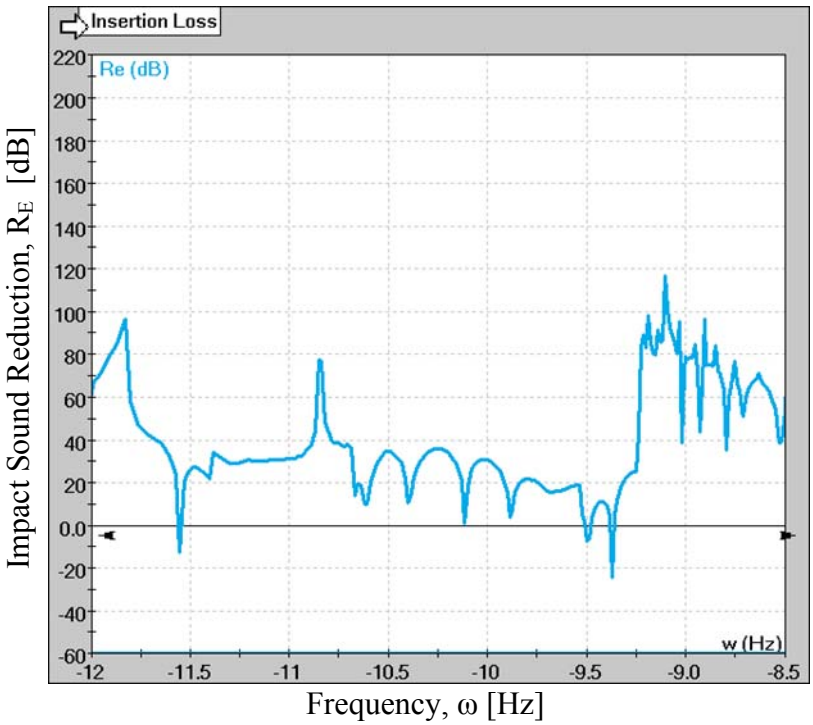

Figure 18 – Impact Sound Reduction vs. Frequency [MDOF]

CHAPTER 4 – Conclusion

A literature review on floor attenuation models for impact structure-borne sound was conducted. Efforts to quantify the human footstep as a vibration source were included, as well as both closed-form and discrete impact sound prediction methods have been presented. The application of these methods to both standard and floating floors revealed that timber-only structures possess innate attenuation properties which must be accounted for in order to achieve accurate prediction of impact sound reduction.

The thesis was focused on the use of vibration isolation as a means of predicting the impact sound insulation provided by floating floors with timber load-bearing floors and floating slabs. To aid in this investigation, the rigid body dynamics software Working Model 2D® was employed. The software was first tested on a simple vibration isolation case, a SDOF system with a rigid concrete foundation. Results underestimated the resonance frequency of the system. Despite this, the impact sound reduction graph closely matched those found in literature. Therefore, WM2D was deemed an appropriate tool for modeling MDOF timber systems.

The MDOF timber floating floor created in WM2D was composed of the impact source, floating slab, resilient layer, and compliant timber load-bearing floor, each of which was created using geometric and material property data obtained from literature. In

order to model the timber load-bearing floor as a transverse orthotropic beam, five layers were used with differing Young's Modulus values. Resilient layer properties were calculated using equivalent spring constants. The source was modeled by a mass-spring-mass system in order to better represent a footstep source. Analysis of the MDOF system showed an improved impact reduction when taking into account the compliance of timber structures.

Proper footstep modeling is important when assessing impact sound reduction accurately. Therefore, obtaining a forcing function for the impact of human footsteps is necessary in the future, perhaps fitted to graphs obtained from measurement. Future research work may also incorporate a hysteresis model in place of the viscous damper assumption used when modeling the resilient layer in this thesis. Additionally, taking into account soft floor coverings such as carpet can more accurately quantify impact sound reduction.

The main goal of this thesis was to help bridge the gap between the fields of structural dynamics and acoustics by employing WM2D as an analysis tool for both vibration isolation and impact sound reduction. Therefore, future work should address the shortcomings of WM2D, especially when plotting frequency response functions. Other prediction techniques such as experimentation, FEM, or SEA should be used to reinforce and verify results from WM2D, especially with orthotropic materials such as timber.

REFERENCES

REFERENCES

Bard, D., J. Sonnerup, and G. Sandberg. "A Finite Element Solution of Structure-Borne Sound Attenuation for a Lightweight Timber Floor." *Building Acoustics*, 2008: 137-152.

Blauert, J., and N. Xiang. *Acoustics for Engineers: Troy Lectures.* Berlin: Springer, 2008.

Brennan, M.J., and N.S. Ferguson. "Vibration Control." In *Advanced Applications in Acoustics, Noise and Vibration*, by F Fahy and J. Walker, 530-580. London: Spon Press, 2004.

Brunskog, Jonas, and Per Hammer. "Prediction Models of Impact Sound Insulation on Timber Floor Structures; A Literature Survey." *Building Acoustics*, 2000: 89-112.

Clasen, D., and S. Langer. "Finite Element Approach for Flanking Transmission in Building Acoustics." *Building Acoustics*, 2007: 1-14.

Cremer, L., M. Heckl, and B.A.T. Petersson. *Structure-Borne Sound: Structural Vibrations and Sound Radiation at Audio Frequencies.* Berlin: Springer, 2005.

Crocker, M.J., ed. *Handbook of Acoustics.* Wiley-Interscience, 1998.

Ekimov, A., and J.M. Sabatier. "Vibration and sound signatures of human footsteps in buildings." *Journal of the Acoustical Society of America*, 2006: 762-768.

Fahy, F., and J. Walker. *Fundamentals of Noise and Vibration.* London: E & FN Spon, 1998.

Hammer, P., and J. Brunskog. "Vibration Isolation on Lightweight Floor Structures." *Building Acoustics*, 2002: 257-269.

Hopkins, C., and R. Hall. "Impact Sound Insulation Using Timber Platform Floating Floors on a Concrete Floor Base." *Building Acoustics*, 2006: 273-284.

Meirovitch, M. *Fundamentals of Vibrations.* New York: McGraw-Hill, 2001.

Möser, M. *Engineering Acoustics: An Introduction to Noise Control.* Berlin: Springer, 2004.

Natke, H.G., and E.U. Saemann. "Structure-Borne Sound." In *Vibration Problems In Structures*, by H. Bachmann, 56-65. Berlin: Birkhäuser, 1995.

Rossing, T.D. *Springer Handbook of Acoustics.* New York: Springer, 2007.

Scholl, W. "Impact Sound Insulation: The Standard Tapping Machine Shall Learn to Walk!" *Building Acoustics*, 2001: 245-256.

Scholl, W., and W. Maysenhölder. "Impact Sound Insulation of Timber Floor: Interaction between Source, Floor Coverings, and Load Bearing Floor." *Building Acoustics*, 1999: 43-61.

Smith, B.J. *Environmental Physics: Acoustics.* New York: Elsevier, 1971.

Stewart, Michael A., and Robert J.M. Craik. "Impact Sound Transmission through a floating floor on a concrete slab." *Applied Acoustics*, 2000: 353-372.

Tadeu, A., A. Pereira, L. Godinho, and J. António. "Prediction of airborne sound and impact sound insulation provided by single and multilayer systems using analytical expressions." *Applied Acoustics*, 2007: 17-42.

Wachulec, M., P.H. Kirkegaard, and S.R.K. Nielsen. "Methods of Estimation of Structure

Borne Noise in Structures - Review." *Structural Dynamics, Paper No. 20*, 2000: 1-17.

Wang, Shih-Liang. "Software Review: Motion Simulation with Working Model 2D and MSC.visualNastran 4D." *Working Model 2D - Reviews and Awards.* http://www.design-simulation.com/wm2d/success/wm2dsoftwarereview.pdf (accessed April 10, 2009).

Warnock, A.C.C., and W. Fasold. "Sound Insulation: Airborne and Impact." In *Handbook of Acoustics*, by M.J. Crocker, 953-984. New York: Wiley-Interscience, 1998.

Wuyts, D., C. Crispin, B. Ingelaere, and M. Van Damme. "Laboratory Sound Insulation Measurements of Improved Timber Floor Constructions: A Parametric Survey." *Building Acoustics*, 2006: 311-325.

CURRICULUM VITAE

Nouri Hacene-Djaballah obtained his B.S. degree in Civil Engineering from George Mason University in 2007. While pursuing a M.S. degree in the same field at GMU, he became an Engineer-in-Training (EIT) and worked as a graduate teaching assistant in mechanics of materials, structural analysis, and structural design. As an active member of GMU's American Society of Civil Engineers (ASCE) chapter, he led the structural analysis and design portion of their first Student Steel Bridge Competition in late 2008 to early 2009. In 2006, Nouri interned at Ross, France, and Ratliff Ltd., a civil engineering design and land surveying firm in Manassas, VA.